Electromagnetically induced spatial-temporal structure of seismicity

Article in Izvestiya Physics of the Solid Earth · June 2005

3 authors, including:

Vladimir Zeigarnik
Joint Institute for High Temperatures
64 PUBLICATIONS **149** CITATIONS

SEE PROFILE

E. B. Fainberg
Russian Academy of Sciences
145 PUBLICATIONS **648** CITATIONS

SEE PROFILE

Some of the authors of this publication are also working on these related projects:

Project #14-05-00756 "Physical simulation of electromagnetic triggering phenomena in areas of discontinuities of rocks under critical stressed conditions" supported by Russian Foundation for Basic Research View project

Удусекщьфптуешс ыщгтвштп ща еру Уфкерэы штеукшщк View project

Electromagnetically Induced Spatial–Temporal Structure of Seismicity

A. A. Avagimov*, V. A. Zeigarnik*, and E. B. Fainberg**

*Institute of Thermophysics of Extreme States, Joint Institute of High Temperatures,
Russian Academy of Sciences, Izhorskaya ul. 13/19, Moscow, 127412 Russia
**Institute of Electromagnetic Research, Schmidt Institute of Physics of the Earth,
Russian Academy of Sciences, Troitsk, Moscow oblast, Russia
Received June 4, 2004

Abstract—New procedures improving the accuracy and informativeness of seismicity analysis are applied to treatment of seismicity recorded in the Bishkek geodynamic research area in periods of the MHD generator operation. The presence of a correlation between MHD starts and seismicity is confirmed. Electromagnetically induced seismicity is generally observed as a higher flow of earthquakes of the class $K = 7$ in a local seismogenic zone surrounding the electromagnetic field source. The electromagnetic input energy is shown to be comparable with that of the induced seismicity. The seismicity structure associated with the MHD generator operation is investigated. The distributions of electromagnetic fields, currents, mechanical stress densities, and the heat flux induced by ground MHD pulses are modeled to gain insight into the spatial scale of electromagnetic effects.

INTRODUCTION

The problem of seismicity induced in a geophysical medium by an external action has been widely discussed in the scientific literature [*Induced Seismicity*, 1994; Tarasov, 1997; Kedrov and Kedrov, 2002; Zakrzhevskaya and Sobolev, 2002; Fainberg *et al.*, 2004]. On the one hand, a fundamental aspect of the study of the coupling mechanism and the induced seismicity is evident, and, on the other hand, this phenomenon opens new possibilities for investigating states and properties of heterogeneous media and, as a consequence, the possibility for controlling the seismic regime. This gave impetus to the study of seismicity induced by the electromagnetic action of a pulsed MHD generator.

Preliminary results of the study of electroseismic coupling effects in the Bishkek geodynamic research area are presented in [Tarasov *et al.*, 1999, 2001]. Their main implication is that the seismicity of this area becomes noticeably higher after the electromagnetic action. Electromagnetic pulses are supposed to initiate the release of tectonically accumulated energy via relatively weak earthquakes. A similar effect was also observed in experiments on acoustic emission in which a cyclic electric action was applied to a sample subjected to biaxial compression [Sobolev *et al.*, 2000].

The importance of these results and the potentialities of the discovered effect call for additional information to be obtained in order to elucidate the elastic field generation mechanism and to construct a model of the seismoelectromagnetic coupling. In this connection, it is appropriate to develop adequate schemes of data treatment for analysis of spatial–temporal characteristics of this phenomenon and the related electromagnetic processes.

TREATMENT OF SEISMICITY INDUCED BY THE IMPULSIVE MHD EFFECT

The structure of induced seismicity is determined not only by the endo- and exogenic factors forming the state of the geophysical medium but also by the discrete mode of an electromagnetic action. The electromagnetic action in a specially planned experiment is, by definition, a controlled procedure, which implies the possibility of the realization of a deterministic response to a cyclic action. In this case, within a chosen sample, one deals with a single input pulse and the response induced by it. Violation of this coupling algorithm leads to ambiguity of results.

MHD pulses generated in a regime determined by the goals of deep electromagnetic sounding in the Bishkek research area [Volykhin *et al.*, 1993] were analyzed in [Tarasov *et al.*, 1999, 2001]. As seen from Fig. 1, the time interval ΔT between input pulses varied from 3–7 days to 20–30 days or more.

We remind the reader that properties of the seismic response are examined within a time sample centered at the pulse generation moment, forming two time windows (before and after this moment), and information accumulated from all samples inside these windows is represented by the parameters m and n, respectively. Then, with a given sample length of 40 days and a varying recurrence time interval of MHD pulses (differing from the 20-day window width), the predating window
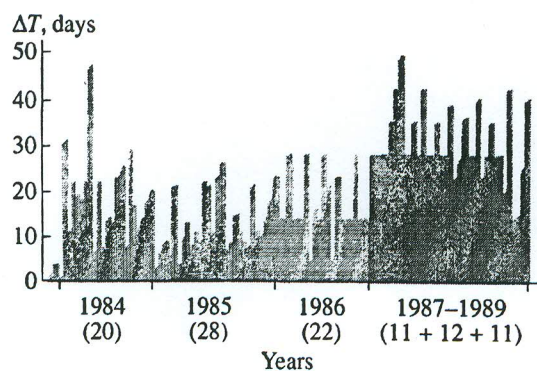
475

ΔT, days

Fig. 1. Discrete regime of the pulsed MHD current. The yearly number of earthquakes is shown in parentheses.

(preceding the time moment of the pulse generation) contains more than one impulsive event; therefore, the adjacent postdating window (following the generation moment) contains information on the seismic response to more than one MHD pulse. The same seismic events fall into predating and postdating time windows associated with different MHD starts, and the total number of earthquakes participating in the analysis exceeds the initial number of seismic events.

It is evident that, with such a scheme of data treatment, the general results of its application are basically incapable of reflecting adequately the structure of the induced seismic response. This refers to both the characteristics of the seismicity distribution inside windows and the comparison of the energy of the induced seismicity with the total energy of the MHD action.

As seen from Fig. 1, 34 MHD generator starts were executed in the period from 1987 through 1989, and 31 of them were separated by intervals of no less than 28 days. Therefore, a 14-day width of the stacking window was chosen as the value optimal for the regime of the MHD generator operation in this period. Results of the application of this scheme to seismicity analysis for the period 1987–1989 are presented below.

Now, we address the second methodological aspect of the data treatment scheme, the determination of an effective spatial scale of the seismoelectromagnetic coupling. Various spatial scales are possible. For example, Tarasov *et al.* [1999, 2001] analyzed seismicity mainly in the area (41°–45° N, 74°–81° E) defined from the earthquake catalog [Mikhailova *et al.*, 1990]. Note that the dipole exciting the electromagnetic field was located at the point (42.69° N, 74.68° E) near the western boundary of this area. Evidently, the seismicity analysis in the entire area (41°–45° N, 74°–81° E), on the one hand, increases statistics but, on the other hand, decreases the definiteness of inferences concerning physical factors responsible for the distributions obtained. Another variant consists in the subdivision of the entire region into smaller areas with the subsequent analysis and comparison of results. A third variant can

be based on the tectonic structure of the region or on its seismotectonic assessment. Modeling of the electromagnetic and elastic fields induced by an MHD generator and their coupling could also be useful.

SEISMICITY STRUCTURE AND ITS CORRELATION WITH AN ELECTROMAGNETIC ACTION

The main area subjected to analysis in our work is the rectangle (41°–44° N, 74°–76° E) denoted as A1, which includes the Bishkek and Kochkorskaya seismogenic zones. This choice decreases the bias of the region relative to the dipole position. For comparison, we also analyzed data in the adjacent rectangle A2 (41°–44° N, 76°–78° E) and in the rectangle A3 (41°–44° N, 74°–78° E) uniting the areas A1 and A2.

The parameter n/m as a function of the earthquake class is plotted in Fig. 2a for the three chosen areas. Here, m is the number of earthquakes of a given class determined from all windows preceding MHD starts and n is their number determined from all windows following the starts; the window width was chosen equal to 14 days. The bars in the A1 plot characterize the determination stability of the ratio n/m, but the technique of their determination differs from that used for the evaluation of standard errors. The point is that, with the exception of classes 6, 7, and 8, the number of earthquakes that occurred in 1987–1989 is small and inadequate for estimating determination uncertainties in n/m values. The estimates presented in the column "limits" of the table (for A1) and shown by bars in Fig. 2a were obtained from the following considerations.

According to the formal technique applied here, the induced seismicity is defined, in accordance with the definition, by postdating windows, and the background seismicity is distributed, on the whole, randomly within both types of windows. It may be supposed that, for some reasons, an event is included into a predating window instead of a postdating one or vice versa. It is evident that such an error will not change significantly the n/m estimate if the statistics is sufficiently large, but the result can be strongly biased if the statistics is small. In accordance with these considerations, the bars shown in the A1 plot (Fig. 2a) were calculated as $(n/m)_{min} = (n-1)/(m+1)$ and $(n/m)_{max} = (n+1)/(m-1)$ without changing the total number of events within a given class ($m + n = const$). It is evident that uncertainties estimated in this way are somewhat tentative.

Now, we compare the seismicity distributions obtained in the areas A1, A2, and A3. The table shows that the ratio between the total numbers of earthquakes of all classes after and before MHD starts is close to unity for the areas A2 and A3 (respectively, 0.99 and 1.07); this is evidence for the absence of any correlation of seismicity with the MHD generator operation within the area A2 and for a weak correlation in the entire area. The ratios n/m for $K \geq 9$ are seen to differ from the aver-

age, but a high error level (table) does not allow us to consider this result as significant.

Now, we address the distribution of the parameter n/m for earthquakes in the area A1 (Fig. 2a). An increase in the number of seismic events of the class $K = 7$ in the postdating window (by 34) is clearly observed. Similar changes are not observed in other cases. It is noteworthy that the total number of earthquakes in the area A1 is also larger in the postdating window, which can be naturally associated with the aforementioned increase in the number of $K = 7$ events but indicates a weak dependence of this fact on the distribution of $K \geq 9$ events.

The detailed distribution of n/m as a function of K (with K varying from 6 to 8.5 with a step of 0.5) plotted in Fig. 2b also supports the aforesaid.

Maps showing epicenters of $K = 7$ earthquakes that occurred in the Bishkek research area (A1) in 14-day intervals before and after MHD pulses are presented in Fig. 3. Epicenters of earthquakes ascribed, according to their occurrence time, to predating windows are traceable along clearly defined lines that can be identified, in a first approximation, with boundaries of heterogeneities (faults). This pattern is also recognizable, albeit less distinctly, in the distribution of epicenters of earthquakes postdating an MHD pulse. Naturally, the total activity of $K = 7$ earthquakes is significantly higher in the postdating window.

The seismicity variation with time is illustrated in Fig. 4. The total daily number of earthquakes in the postdating window n_i is normalized to the average of daily numbers of events m over all predating windows, i.e., to the background level. A maximum exceeding the background level by a factor of 2.1 is observed in the area A1 on the third day after MHD action. Variations in this parameter in the areas A2 and A3 are insignifi-
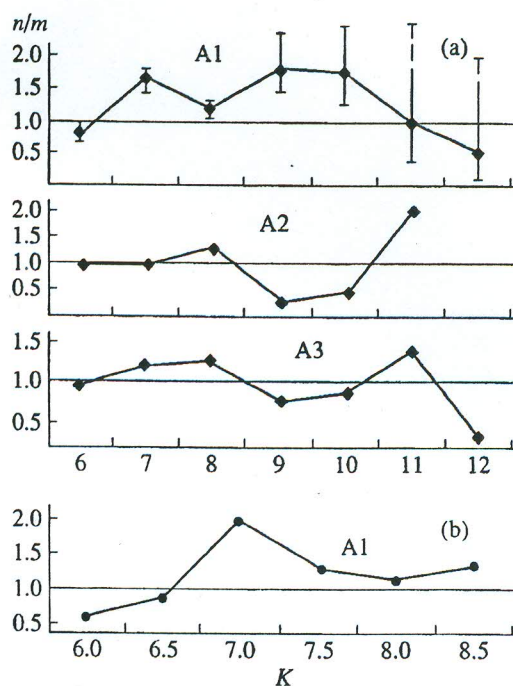

Fig. 2. The energy class (K) dependence of the ratio between the numbers of earthquakes that occurred in the areas A1, A2, and A3 before and after MHD generator starts.

cant and virtually indistinguishable from the background. An increase in seismic activity is also noted on the 13th to 14th days after an MHD pulse, but this interesting feature needs additional analysis and verification.

Table

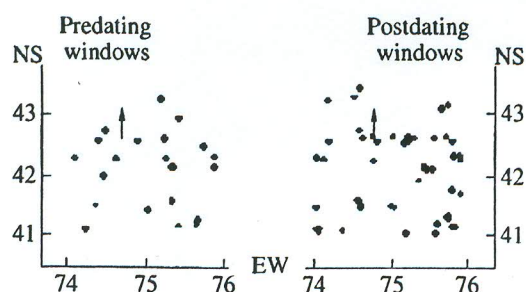| A1					A2				A3			
K	m	n	n/m	limits	K	m	n	n/m	K	m	n	n/m
5	3				5	14	18	1.28	5	17	18	1.06
6	9	32	0.82	0.78–0.87	6	123	121	0.98	6	162	153	0.94
7	51	85	1.67	1.61–1.72	7	129	126	0.98	7	180	211	1.17
8	32	38	1.19	1.12–1.26	8	32	41	1.28	8	64	79	1.23
9	5	9	1.8	1.33–2.5	9	11	3	0.27	9	16	12	0.75
10	4	7	1.75	1.2–2.67	10	9	4	0.44	10	13	11	0.85
11	2	2	1	0.33–3.0	11	1	2	2	11	3	4	1.33
12	2	1	0.5	0–2	12	1			12	3	1	0.33
13					13		1		13		1	
	138	174	1.26	1.24–1.27		320	316	0.99		458	490	1.07

Fig. 3. Distribution of epicenters of $K = 7$ earthquakes in predating and postdating windows. The position of the MHD dipole is shown by an arrow.
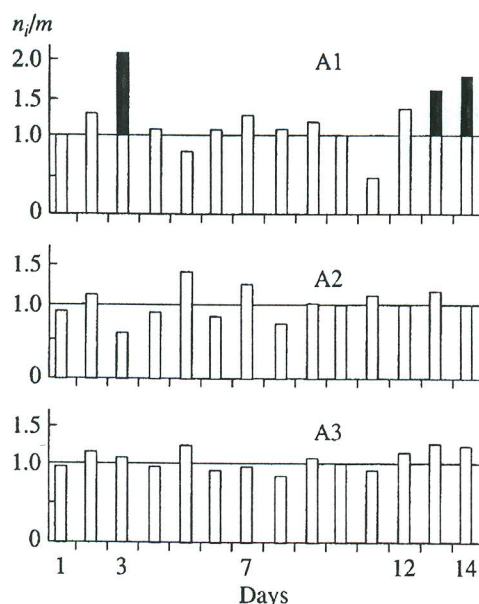

Fig. 4. Distribution of the daily number of earthquakes in the postdating window.

STRUCTURE OF THE SPATIAL MHD-INDUCED DISTRIBUTIONS OF CURRENTS, PONDEROMOTIVE FORCES, AND HEAT FLUXES IN THE EARTH

The seismic activity increase effect of MHD pulses in the range of the earthquake classes 6–8, observed previously and supported by the results presented above, is important and its origin needs to be elucidated. Numerical modeling of heat fluxes induced by sudden commencement magnetic storms [Fainberg *et al.*, 2004] showed that the magnetic storm energy released in the form of heat is comparable with the energy released by earthquakes. Most heat is released in the upper 10–20 km of the section and concentrates at faults. However, simple estimates of heating of rocks involved in this process show that significant heating of the section requires millions of years even if this process is adiabatic.

Several essential features characterize investigations of the tectonic effects of magnetic storms and MHD pulses. Magnetic storms arise permanently and are global phenomena irregular in time. They are uncontrollable. MHD pulses are advantageous in this respect: the source of the current excited by the MHD generator is a 4.2-km grounded line, and MHD starts are controllable. These distinctions, along with the established correlation between seismicity and the action of MHD pulses, suggest that additional constraints on the origin and spatial distribution of this effect can be gained from modeling of the distributions of electromagnetic fields and heat fluxes induced by an MHD generator.

A 3-D regional geoelectric model of the South Tien Shan, including the Bishkek research area and its vicinity, was constructed in [Fainberg *et al.*, 2004] with the use of published geological and geophysical data including geologic and tectonic maps and reconstructions of the region, as well as results of magnetotelluric, frequency, and d.c. soundings described in detail in [Volykhin *et al.*, 1993; Trapeznikov *et al.*, 1997]. Although this model is not comprehensive enough to be used in detailed modeling of the electromagnetic field generated by an MHD generator, it is suitable for the determination of general regional characteristics of MHD-induced electromagnetic and thermal fields and the estimation of the size of the area affected by these fields.

The 160×170-km region shown in Fig. 5 [Volykhin *et al.*, 1993] was chosen for modeling. A current "dipole" is located immediately at the boundary between the Mesozoic–Cenozoic deposits of the Chu depression and outcrops of pre-Mesozoic deposits. In the dipole area, the upper part of the section (to a depth of about 5 km) is represented by relatively high resistivity (80–300 Ω m) rocks. They overlie a crustal conductor (14 Ω m) extending to a depth of about 10 km. High resistivity rocks occur at greater depths.

As is shown below, MHD pulses have a low frequency spectrum and, therefore, modeling of the general distribution patterns of the electromagnetic and thermal fields can be restricted to the class of thin layer models, in which a heterogeneous layer is represented by a thin layer of an electrical conductivity $S(x, y)$ confined to the boundary of a layer in a layered section.

The model consists of six horizontal homogeneous layers: $h_1 = 2$ km, $\rho_1 = 100 \, \Omega$ m; $h_2 = 3$ km, $\rho_2 = 100 \, \Omega$ m; $h_3 = 5$ km, $\rho_3 = 100 \, \Omega$ m; $h_4 = 5$ km, $\rho_4 = 20 \, \Omega$ m; $h_5 = 10$ km, $\rho_5 = 300 \, \Omega$ m; and $\rho_6 = 1000 \, \Omega$ m. The distributions $S_n(x, y)$ were constructed from geoelectric structures along profiles I–III and at individual points of inductive and transient electromagnetic soundings with the use of interpolation taking into account the geology and tectonics of the region. Maps showing S values in the four upper inhomogeneous thin layers at depths of 0 km (S_1), 2 km (S_2), 5 km (S_3), and 10 km (S_4) are presented in Fig. 6.
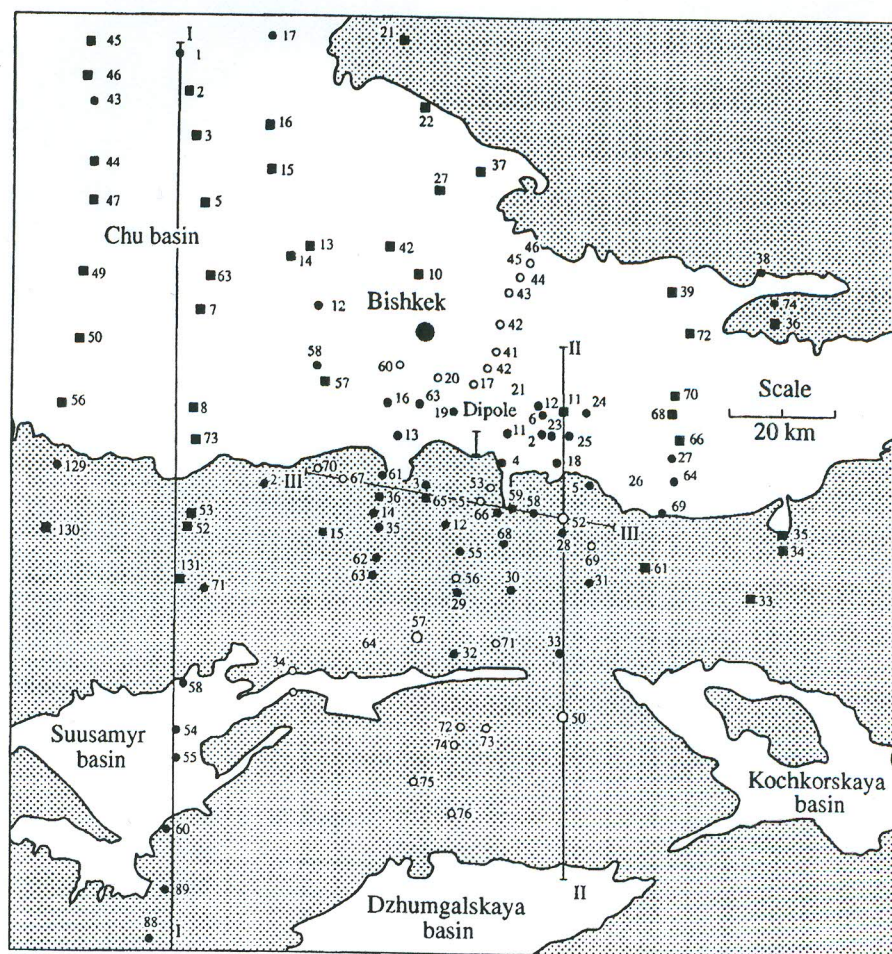
Fig. 5. Schematic map of the Bishkek research area and the adjacent territory. Lines I–I, II–II, and III–III are EM sounding profiles. The squares are MTS stations, the solid circles are frequency and transient electromagnetic sounding points, and the dipole is the electric line of the MHD generator.

Calculations were performed for a typical MHD pulse shown in Fig. 7a. Its spectrum is presented in Fig. 7b and shows that the modeling can be restricted to the frequency range $1 < \omega < 100 \text{ s}^{-1}$. The electromagnetic field was calculated by the modified iterative-dissipative method [Singer, 1995; Singer and Fainberg, 1999]. Figure 8a presents the distribution of the horizontal component of the current density at a depth of 5 km in the phase of maximum amplitudes of the source current. As seen from the figure, the current density j reaches $8 \times 10^{-3} \text{ A/m}^2$ near the source, rapidly decreases away from the source, and does not exceed 10% of its maximum value at distances of 10–15 km and a few fractions of percent at the boundaries of the modeling area. Thus, the MHD generator activates earthquakes within an area more than 2–3 times larger than the area of the current spreading.

Now, we address other fields related to the propagation of telluric currents. First of all, it is natural to suggest that currents excited in the Earth have a ponderomotive effect on rocks. The value $d\mathbf{f}$ of this force produced by an element $d\mathbf{I}$ of the telluric current excited by an MHD pulse can be readily estimated as $\mathbf{f} = [d\mathbf{I} \times \mathbf{B}_0]$, where I is the current and $\mathbf{B}_0$ is the main geomagnetic field in the Bishkek research area. Figure 8b shows the distribution of densities of horizontal stresses (N/m^2) at a depth of 2 km. The stress pulses are seen to be small within an area of 1 m^2, but their integral value for the entire research area can be significant. Evidently, the stresses can reach the highest values in the most conductive zones, namely, faults filled with loose water-saturated deposits. In order to estimate their possible values, more detailed 3-D modeling of an $\sim 20 \times 20 \times 10$-km region should be performed. The question of how much these stresses exceed those accumulated during earthquake nucleation needs special consideration and is beyond the scope of this paper.
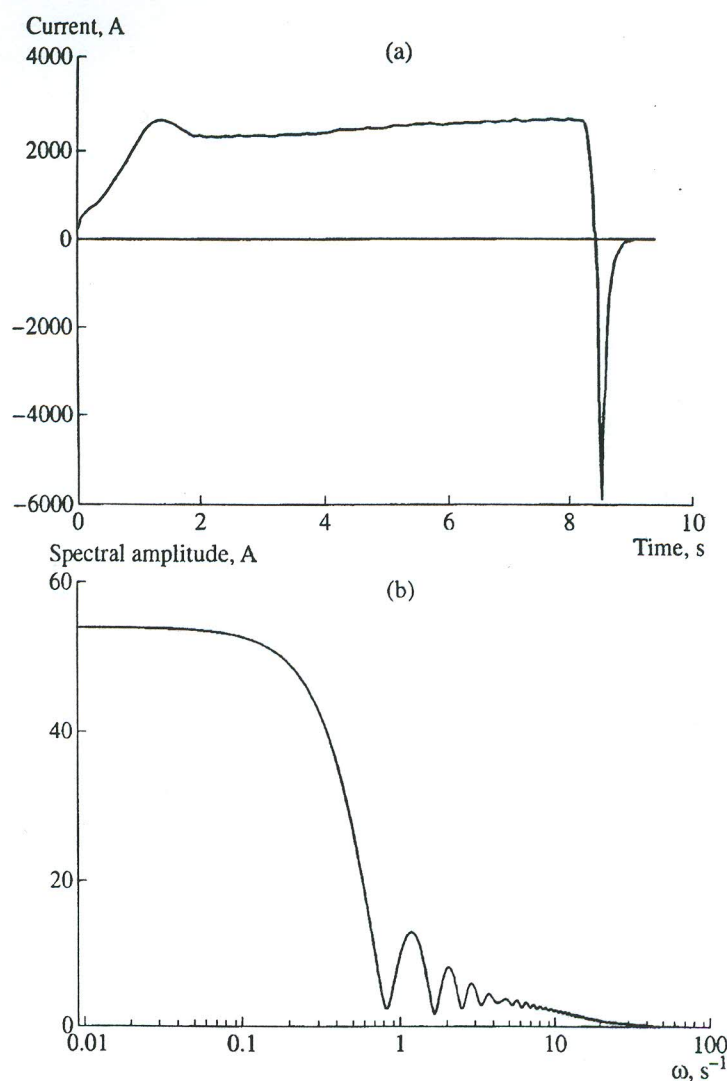
Fig. 7. MHD generator current pulse (a) and its spectrum (b).

As seen from Fig. 9, the heat flux concentrates in the 5-km-thick shallow layer within distances no greater than several lengths of the current cable. The heat flux outside this area is insignificant. Heat fluxes near the MHD source are comparable in value with the fluxes generated by magnetic storms; however, as distinct from the storms, exciting only vertical heat fluxes, the MHD generator creates fluxes propagating also in the horizontal direction, and they are comparable in value with the vertical fluxes. It is noteworthy that, notwithstanding sharp contrasts in the electrical conductivity near the dipole, the distribution of heat fluxes within 5 km from the dipole is symmetric and weakly distorted by the conductivity inhomogeneities.

DISCUSSION

Seismicity is nearly always treated in terms of the parameters of spatial distribution of earthquakes. This is particularly relevant to the case of seismicity induced by electric currents, which depends, by definition, on the distance from the excitation source. The effect of MHD generator current pulses is spatially local; this basic conclusion follows from the structure of the heat fluxes analyzed in this work. The heat fluxes induced by current pulses are related to the inferred geoelectric inhomogeneities. A similar pattern is observed in the distributions of stresses and electric current densities. This supports the correctness of the choice of an area appropriate for the search for possible seismicity changes.
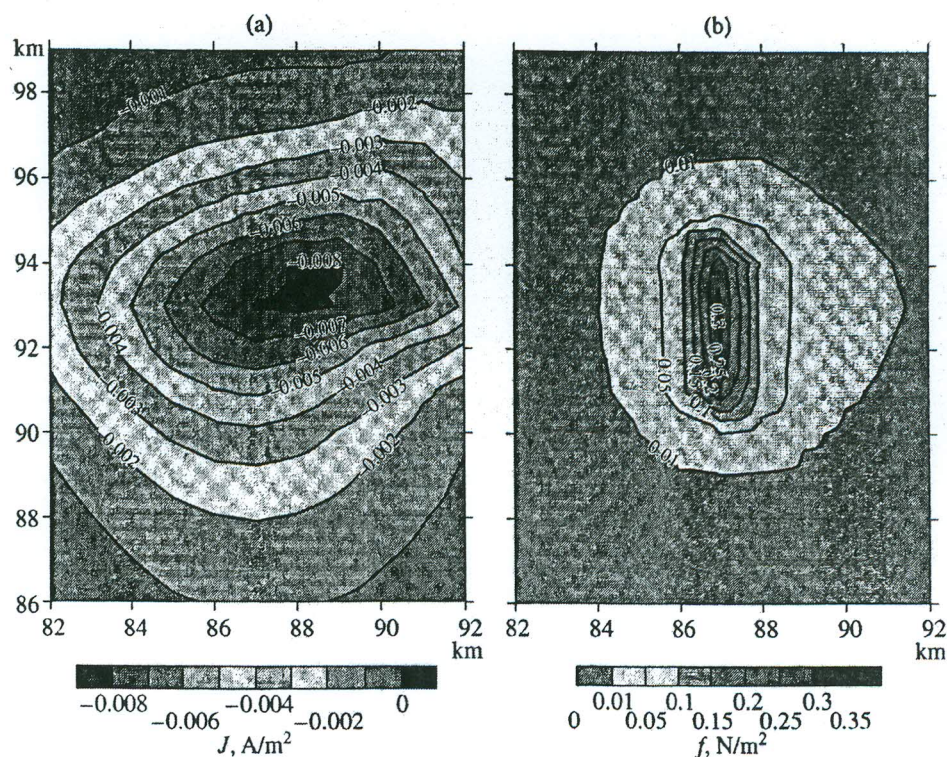
Fig. 8. Distributions of the densities of the electric current (a) and stresses (b) at a depth of 5 km.

The results obtained in this work show that, in the Bishkek research area, MHD input pulses activate seismicity dominated by earthquakes of the energy class $K = 7$. Epicenters of earthquakes that occurred before and after electric actions are associated with the inferred geoelectric contrasts but also gravitate toward the excitation dipole, indicating that the process of formation of induced seismicity is evidently local in space and is confined to the Bishkek and Kochkorskaya seismogenic zones within the rectangle ($41°$–$44°$ N, $74°$–$76°$ E). No significant changes are observed in the adjacent area (see table).

The 14-day sample analysis conducted with due regard for the discrete mode of electric current pulses revealed a seismicity maximum 3 days after MHD starts and a significant increase in the ratio n/m on the 12th to 14th day.

In principle, the results of comparison of the induced seismicity energy with the total energy of the MHD action depend on the data processing scheme, in particular, on the size of the territory studied. The number of events and, accordingly, their total energy in sampling windows increase with the area size, but the energies of the external MHD action and the induced seismicity remain unchanged. Since the background seismicity distribution within windows is random before and after the MHD action and "the daily number of earthquakes is highly variable within a year"

[Kedrov and Kedrov, 2002], enlargement of the background seismicity base can lead to overestimated results of comparison between these energies and, in the general case, to their ambiguity.

The total energy delivered by the MHD generator into the medium over the period from 1987 through 1989 is 5.7×10^8 J, and the energy level of induced seismicity (A1) is on the order of 9.5×10^8 J for earthquakes of $K \leq 8$. We should note a nearly cyclic pattern of the MHD action in the period from 1987 through 1989, with the average pulse energy being $(1–2) \times 10^7$ J. The induced seismicity is mainly realized via earthquakes of $K = 7$ ($E_7 = 1 \times 10^7$ J). Without regard for energy losses associated with the MHD action and conversion processes, the energy released by earthquakes is comparable with that of the electric action: their difference is within one order of magnitude. According to the table (A1), the total number of earthquakes and their numbers in various energy classes related to the induced seismicity support, on the whole, the above.

The effect of electric currents on all of the fields considered above (stress density, electric current density, heat fluxes, and induced seismicity) is highest within the inferred heterogeneities and in the depth range 0–5 km, i.e., within the hydrostatic crustal zone, whose fractures, pores, and cavities are typically filled with free or bound water.
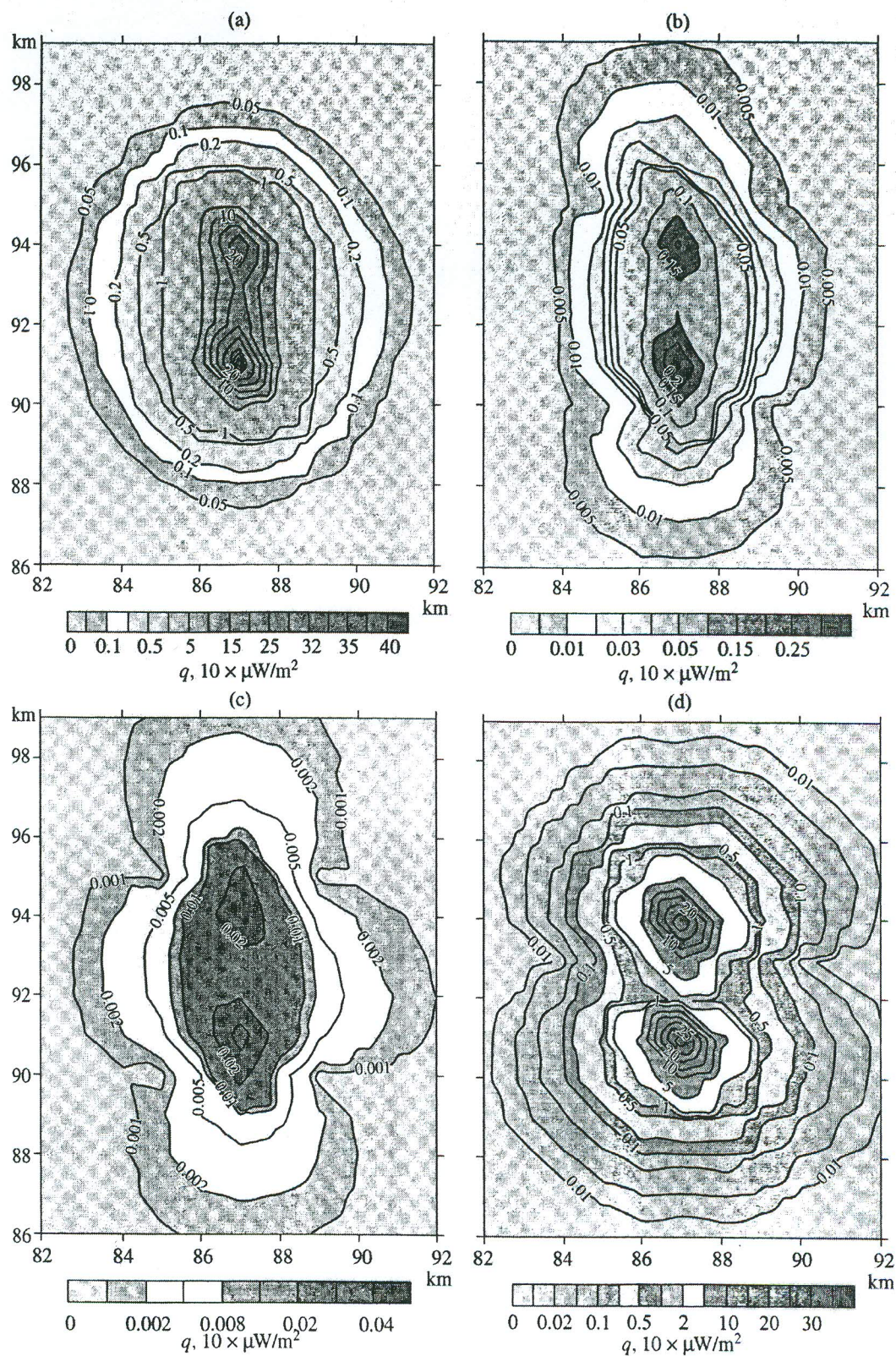
Fig. 9. Distributions of the vertical heat flux at depths of (a) 0, (b) 2, and (c) 5 km and (d) the distribution of the horizontal heat flux.

A model using electrical characteristics of the medium and its energy content as a factor responsible for the generation of an anomalous elastic field in response to an electrical action was discussed in [Avagimov and Zeigarnik, 2002]. The response of the medium to electromagnetic actions is selective, being most pronounced in heterogeneous fluid-saturated regions. This can be primarily due to a high level of free electric charges and an electrokinetic potential [Grigorov, 1973] typical of highly dispersed and fluid-saturated media. In real energetically active media, the action of ponderomotive forces transforms an area of double electrical layers into a thermodynamically unstable zone [Balasanyan, 1990], creating pressure gradients in a fluid and thereby macroscopic mechanical disturbances, and redistributes structural stresses in the medium, which leads to a redistribution and subsequent release of elastic energy at fractures with a critical level of energy content.

The comparable energies of the electrical input action and the induced seismicity are evidence favoring the seismoelectromagnetic coupling scheme proposed in this paper. However, a complete understanding of the origin of the discovered correlation calls for new experiments.

CONCLUSIONS

The method applied here to the analysis of earthquake and MHD pulses provided additional constraints on the seismicity structure induced by an electromagnetic input action in the Bishkek geodynamic research area. Modeling of spatial distributions of the electric current density, stresses, and heat fluxes excited by MHD pulses refined the limiting spatial scale of seismoelectromagnetic coupling.

It has been established that the induced seismicity is realized as a higher earthquake flow dominated by events of the class $K = 7$ in a local seismogenic zone adjacent to the dipole exciting the electromagnetic field. The energies of the electric action and the induced seismicity are shown to be comparable.

ACKNOWLEDGMENTS

REFERENCES

1. A. A. Avagimov and V. A. Zeigarnik, "On a Possible Mechanism of Formation of Caused Seismicity Induced by Electromagnetic Impact," in *III International Workshop on Magnetic, Electric and Electromagnetic Methods in Seismology and Volcanology. Abstracts* (Moscow, 2002), pp. 95–98.

2. S. Yu. Balasanyan, *Dynamic Geoelectrics* (Nauka, Novosibirsk, 1990) [in Russian].

3. E. B. Fainberg, "Global Geomagnetic Sounding," in *Mathematical Modeling of Electromagnetic Fields* (IZMIRAN, 1983), pp. 79–121 [in Russian].

4. E. B. Fainberg, A. A. Avagimov, V. A. Zeigarnik, and T. A. Vasil'eva, "Generation of Heat Flows in the Earth's Interior by Global Geomagnetic Storms," Fiz. Zemli, No. 4, 54–62 (2004) [Izvestiya, Phys. Solid Earth **40**, 315–322 (2004)].

5. O. N. Grigorov, *Electrokinetic Phenomena* (LGU, Leningrad, 1973) [in Russian].

6. *Induced Seismicity* (Nauka, Moscow, 1994) [in Russian].

7. O. K. Kedrov and E. O. Kedrov, "The Influence of Underground Nuclear Explosions on Regional Seismicity," Fiz. Zemli, No. 3, 21–34 (2002) [Izvestiya, Phys. Solid Earth **38**, 194–206 (2002)].

8. N. N. Mikhailova *et al.*, *Catalog of Earthquakes in the North Tien Shan and Adjacent Territories for the Period 1975–1982* (Nauka, Alma-Ata, 1990), Parts 1 and 2 [in Russian].

9. B. Sh. Singer, "Method for Solution of Maxwell's Equations in Non-Uniform Media," Geophys. J. Int. **20**, 590–598 (1995).

10. B. Sh. Singer and E. B. Fainberg, "Modeling of Electromagnetic Fields in Thin Heterogeneous Layers with Application to Field Generation by Volcanoes—Theory and Examples," Geophys. J. Int. **138**, 125–145 (1999).

11. G. A. Sobolev, A. V. Ponomarev, A. A. Avagimov, and V. A. Zeigarnik, "Initiating Acoustic Emission with Electric Action," in *27th General Assembly of the European Seismological Commission (ESC), Lisbon, Portugal, September 10–15, 2000*, p. 17.

12. N. T. Tarasov, "Variation in Crustal Seismicity Due to an Electric Action," Dokl. Ross. Akad. Nauk **353** (4), 542–545 (1997).

13. N. T. Tarasov, N. V. Tarasova, A. A. Avagimov, and V. A. Zeigarnik, "The Effect of Powerful Electromagnetic Pulses on Seismicity in Central Asia and Kazakhstan," Vulkanol. Seismol., No. 4/5, 152–160 (1999).

14. N. T. Tarasov, N. V. Tarasova, A. A. Avagimov, and V. A. Zeigarnik, "Electromagnetically Induced Variation in Seismicity in the Bishkek Geodynamic Research Area," Geol. Geofiz. **42** (10), 1641–1649 (2001).

15. Yu. A. Trapeznikov, E. V. Andreeva, V. Yu. Batalev, *et al.*, "Magnetotelluric Sounding in the Kyrgyz Tien Shan Mountains," Fiz. Zemli, No. 1, 3–20 (1997).

16. A. M. Volykhin, V. D. Bragin, A. V. Zubovich, *et al.*, *Signatures of Geodynamic Processes in Geophysical Fields* (Nauka, Moscow, 1993) [in Russian].

17. N. A. Zakrzhevskaya and G. A. Sobolev, "On the Seismicity Effect of Magnetic Storms," Fiz. Zemli, No. 4, 3–15 (2002) [Izvestiya, Phys. Solid Earth **38**, 249–261 (2002)].